





Article

# Sentinel 2 Analysis of Turbidity Patterns in a Coastal Lagoon

María-Teresa Sebastiá-Frasquet <sup>1,\*</sup>, Jesús A. Aguilar-Maldonado <sup>2</sup>,  
Eduardo Santamaría-Del-Ángel <sup>2</sup> and Javier Estornell <sup>3</sup>

<sup>1</sup> Instituto de Investigación para la Gestión Integrada de Zonas Costeras, Universitat Politècnica de València, C/Paraninfo, 1, 46730 Grau de Gandia, Spain

<sup>2</sup> Facultad de Ciencias Marinas, Universidad Autónoma de Baja California, Ensenada 22860, Mexico; [jesusaguilarmaldonado@gmail.com](mailto:jesusaguilarmaldonado@gmail.com) (J.A.A.-M.); [santamaria@uabc.edu.mx](mailto:santamaria@uabc.edu.mx) (E.S.-D.-Á.)

<sup>3</sup> Grupo de Cartografía GeoAmbiental y Teledetección, Universitat Politècnica de València, Camí de Vera s/n, 46022 Valencia, Spain; [jaescres@upv.es](mailto:jaescres@upv.es)

\* Correspondence: [mtsebastia@hma.upv.es](mailto:mtsebastia@hma.upv.es)

Received: 7 October 2019; Accepted: 4 December 2019; Published: 6 December 2019



**Abstract:** Coastal lagoons are transitional ecosystems with complex spatial and temporal variability. Remote sensing tools are essential for monitoring and unveiling their variability. Turbidity is a water quality parameter used for studying eutrophication and sediment transport. The objective of this research is to analyze the monthly turbidity pattern in a shallow coastal lagoon along two years with different precipitation regimes. The selected study area is the Albufera de Valencia lagoon (Spain). For this purpose, we used Sentinel 2 images and in situ data from the monitoring program of the Environment General Subdivision of the regional government. We obtained Sentinel 2A and 2B images for years 2017 and 2018 and processed them with SNAP software. The results of the correlation analysis between satellite and in situ data, corroborate that the reflectance of band 5 (705 nm) is suitable for the analysis of turbidity patterns in shallow lagoons (average depth 1 m), such as the Albufera lagoon, even in eutrophic conditions. Turbidity patterns in the Albufera lagoon show a similar trend in wet and dry years, which is mainly linked to the irrigation practice of rice paddies. High turbidity periods are linked to higher water residence time and closed floodgates. However, precipitation and wind also play an important role in the spatial distribution of turbidity. During storm events, phytoplankton and sediments are discharged to the sea, if the floodgates remain open. Fortunately, the rice harvesting season, when the floodgates are open, coincides with the beginning of the rainy period. Nevertheless, this is a lucky coincidence. It is important to develop conscious management of floodgates, because having them closed during rain events can have several negative effects both for the lagoon and for the receiving coastal waters and ecosystem. Non-discharged solids may accumulate in the lagoon worsening the clogging problems, and the beaches next to the receiving coastal waters will not receive an important load of solids to nourish them.

**Keywords:** Sentinel; Secchi disk; chlorophyll *a*; sediments; phytoplankton

## 1. Introduction

Coastal lagoons are transitional ecosystems between inland and coastal waters. They are shallow water bodies separated from the ocean by a barrier and connected, at least intermittently, to the ocean by one or more restricted inlets [1]. Given these characteristics, they exhibit complex spatial and temporal variability. They are usually part of wetland ecosystems and are among the most endangered ecosystems, especially in coastal areas, due to several anthropogenic threats [2]. These ecosystems are characterized by a high variability due to both natural intrinsic variability and anthropic pressures

variability (e.g., man-controlled hydrological cycle, wastewater discharge, etc.). In situ monitoring programs (e.g., Water Framework Directive) have difficulty diagnosing their quality status and the effectiveness of restoration measures. Remote sensing is a complementary tool to the traditional on-site approach that allows constructing a synoptic view that is not possible otherwise. During the last decades, several studies have aimed at monitoring indicator parameters of water quality both in inland and in coastal waters using satellite images. However, the spatial and temporal scale have been constraints for small sized and highly variable ecosystems such as coastal lagoons. High temporal resolution sensors (1–3 days) such as Moderate Resolution Imaging Spectroradiometer (MODIS) or MEdium Resolution Imaging Spectrometer (MERIS) have a limited spatial resolution (250/500 m). Higher spatial resolution sensors such as Landsat Thematic Mapper (TM) (30 m) or SPOT have a low temporal resolution (16 days) not enough for the highly dynamic coastal lagoons [3,4]. The Copernicus Sentinel-2 mission of the European Space Agency (ESA) comprises a constellation of two polar-orbiting satellites, and the first one, Sentinel-2A is operational since June 2015. This mission combines both a high spatial (10–60 m) and a high temporal resolution (5 days) that are necessary to monitor coastal lagoons [4,5].

One of the major environmental problems of coastal lagoons is eutrophication, and one of the most commons parameters used to monitor their ecological status is chlorophyll *a* (Chl*a*) concentration [3,6,7]. Consequently, recent studies have applied the advances in remote sensing to study temporal and spatial evolution of Chl*a* using Sentinel-2 images [8]. A very recent study has applied Sentinel-2 images also to study phycocyanin concentration, which is an indicator of cyanobacterial blooms [7]. Turbidity is also a water quality parameter used as a eutrophication indicator [9]. Turbidity reduces the availability of light underwater, and thus limits light availability for phytoplankton growth and primary productivity [9,10]. Moreover, it is also important for nutrient dynamics, pollutants, and sediment transport [9]. According to the ASTM-International definition, turbidity is an expression of the optical properties of a liquid that causes light rays to be scattered and absorbed rather than transmitted in straight lines through a sample. Turbidity, suspended particulate matter (SPM), and Secchi disk depth are three variables closely related. Frequently, turbidity is used as an estimation of SPM concentration [9,11]. In fact, traditionally, turbidity is estimated visually using a Secchi disk depth or measured directly with nephelometry [10]. The analysis of turbidity is especially important in optically complex waters where phytoplankton and SPM do not covary, and sediment contribution can result in an overestimation of Chl*a* [12,13]. Previous research applied remote sensing to map turbidity in complex coastal waters. The authors of [14] used Landsat 8 and SPOT images in the Mar Menor (Spain); in [4] the authors applied Landsat 5, 7, and 8 in the turbid Gironde and Loire estuaries (France); the authors of [10] used Landsat 8 in Cam Ranh Bay and Thuy Trieu Lagoon (Vietnam), and in [9] the authors applied a multisensory approach in the Danube Delta (Romania). Recently, the trend is to apply Sentinel 2 advantages to monitoring highly variable ecosystems [5,12,13,15].

Determining turbidity in shallow waters requires the use of spectral bands that are sensitive to turbidity and have a limited depth penetration to avoid substantial interference from the bottom [15]. Water absorption increases rapidly from red (645–700 nm) to red edge NIR (700–780 nm) [16]. This absorption limits the light received from the bottom, while it returns light scattered by suspended materials. These bands offer a good balance between turbidity detection and bottom detection [17]. Several studies have already indicated that these spectral bands are appropriate for monitoring turbidity or suspended solids in optically complex regions [15,17,18]. According to [15], the 704 nm wavelength gives the greatest return of light to the sensor at depths between 1 and 2 m. However, at longer wavelengths, sensitivity to suspended material is lost in shallow and very turbid waters [15].

The objective of this research is to analyze the monthly turbidity pattern in a shallow coastal lagoon along two years with different precipitation regime. The selected study area is the *Albufera de Valencia* lagoon (Valencia, Spain). This lagoon faces a eutrophication problem, and it is at risk of disappearing due to the accumulation of sediments. The analysis of turbidity is important to unveil the sediment transport dynamics. For this purpose, we used Sentinel 2 images and in situ data from

the monitoring program of the Environment General Subdivision of the regional government, which has been implemented since year 1995. Remote sensing is the only way to obtain a synoptic view of the entire lagoon due to the high spatial complexity and the varying water quality of the more than 60 tributaries.

## 2. Materials and Methods

### 2.1. Study Area

The *Albufera de Valencia* lagoon is a shallow turbid coastal lagoon, located in the Mediterranean coast, 10 km south of the city of Valencia (Figure 1) [19,20]. It has an average depth close to 1 m (1–3 m) and covers an area of approximately 24 km<sup>2</sup> [6]. This water body is characterized as hypertrophic, with average annual Chla levels of 167 µg L<sup>-1</sup> (4–322 µg L<sup>-1</sup>) and Secchi disk depth of 0.34 m (0.18–1 m) [6].

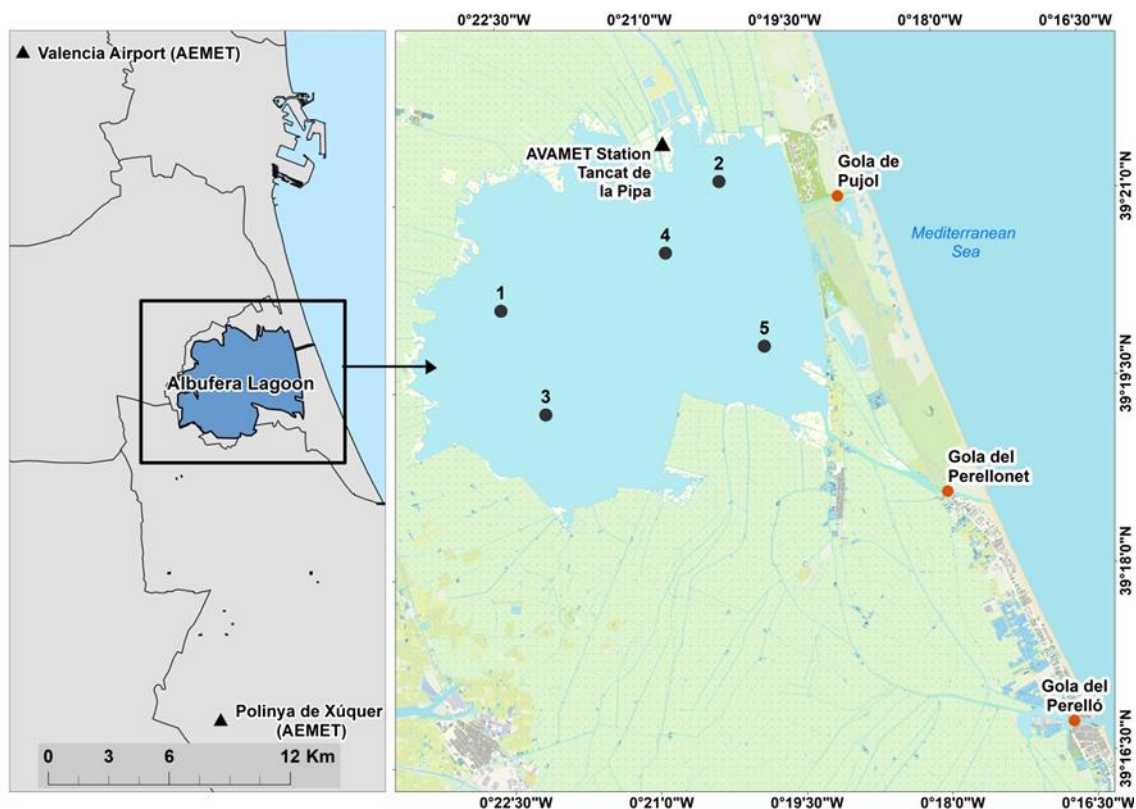


**Figure 1.** Study area, the *Albufera de Valencia* lagoon and surroundings. Numbered black points are sampling stations from the monitoring program of the Environment General Subdivision of the Valencian government.

It is part of the *Albufera de Valencia* coastal wetland, which is one of the most representative wetlands in the Mediterranean basin, and holds several protection figures at national and international level, such as Spanish Natural Park, Special Protection Areas (SPAs) for birds, Sites of Community Importance (SCIs), and Ramsar Site.

The lagoon is surrounded by an agricultural area with an approximate surface of 223 km<sup>2</sup> primarily used for rice cultivation [6]. The local water council, under the direction of farmers, controls the hydrological cycle in the watershed to meet the needs of rice crop [6,8]. Farming contributes about 60% of the inputs to the Albufera through 63 irrigation channels that carry water from the Turia and Júcar rivers [21,22]. Other sources of water are treated wastewater from the urban and industrial areas nearby, groundwater contributions, direct precipitation on the lagoon, and potential indirect contributions of seawater through sea connections [3].

The lagoon is connected to the Mediterranean Sea through three floodgates, “Golas” in Spanish, from North to South, Gola de Pujol, Gola del Perelló, and Gola del Perellonet (Figure 1). The local water council operates them according to the needs of the rice cycle. They are open from January to March to allow the water level of the lagoon to increase for irrigation. During the rice growing season (April–September) the floodgates remain closed to allow field flooding and with an insignificant flow to the lagoon. Gates open in September to allow rice fields to dry for rice harvest. Finally, gates close again in November to allow flooding of harvested rice fields, which favors the mineralization of nutrients [23].

The eutrophication of the lagoon is an old problem that dates back to the 1960s. Since then, the system shifted from a clear state to a turbid stable state that was consolidated by the almost total disappearance of macrophytes in the early 1970s [24]. The turbid state has prevailed since then, although some studies report short clear water events one or twice a year, with *Chla* concentrations below 5 mg/m<sup>3</sup> [6]. In addition, sediment deposition threatens the lagoon with clogging showing the importance of studying turbidity patterns.

## 2.2. Precipitation and Wind Data

The first step was to select one year with total precipitation above the annual average and one year below the annual average, to analyze turbidity patterns in different precipitation regime conditions. The closest stations to the Albufera lagoon with full available data from 1995 to 2018 are the Valencia Airport station (north) and the Polinya del Xúquer station (south), which belong to the State Meteorological Agency (AEMET) (Figure 1). This period was selected because the in situ monitoring data began to be compiled in 1995. Within the Albufera Natural Park, there is a station that belongs to the Valencian Association of Meteorology (AVAMET), called *Tanecat de la Pipa* station. There are available data for this station since 2016. We selected the year 2017 as a year below the average precipitation, and 2018 as a year above the average, comparing the data from *Tanecat de la Pipa* station with historic records. Wind data were obtained from the *Tanecat de la Pipa* station.

## 2.3. Secchi Disk and Suspended Matter

Secchi disk depth (SDD) (cm) and suspended particulated matter (SPM) (mg/L) were measured monthly from 1995 to 2018 by the monitoring program of the Environment General Subdivision of the Valencian government. There are five sampling stations in the Albufera lagoon, shown as dots in Figure 1. These data are available online: <http://www.agroambient.gva.es/es/> (accessed on 6 October 2019).

SDD was measured with a 30 cm diameter black-and-white disk, which was submerged in the water until it was no longer visible to an observer on the surface [25,26]. Secchi disk depth is inversely proportional to the amount of dissolved and/or particulate matter present in the water column; thus, is a turbidity indicator. SPM was determined following the Standard Methods (2005) procedure, 2540D, for surface waters.

SDD and SPM were standardized using the following Equation

$$Z = \frac{x - \bar{x}}{SD}, \quad (1)$$

where  $x$  is the month datum of year  $i$ ,  $\bar{x}$  is the month average from 1995 to 2018, and  $SD$  is the monthly standard deviation from 1995 to 2018.

The standardized values were classified as follows: (1) values in the interval  $(-1, 1)$  indicate normal values; (2) values in the interval  $(1, 1.6)$  are above normal conditions, and (3) values  $(>1.6)$  are highly anomalous. The limit of the anomalous conditions was based on an Inverse Cumulative Distribution Function (ICDF), in a normal distribution, which defines 1.6 standard deviations as the limit of values without noise with 95% confidence [27,28].

Then, the month average of the standardized values from 1995 to 2018 was calculated to characterize each month. The purpose is to characterize the temporal transparency pattern, which depends on the rice cultivation cycle.

#### 2.4. Satellite Data

We obtained Sentinel 2A and 2B images for the years 2017 and 2018 from the Sentinel Scientific Data Hub available online: <https://scihub.copernicus.eu/> (accessed on 6 October 2019) (Table 1). Only cloud-free images were used to observe the spatial variation. The images were subset to the exclusive area of the Albufera lagoon based on a shapefile before further processing.

**Table 1.** List of Sentinel 2A and 2B images used in this study by date. Only cloud-free images were selected.

Year 2018	Year 2017
11 January	16 January
20 February	5 February
27 March	17 March
26 April	16 April
21 May	16 May
20 June	15 June
10 July	10 July
19 August	4 August
13 September	13 September
3 October	13 October
27 November	22 November
22 December	17 December

Software SNAP version 5 (Brockmann Consult) was used for image processing. All images were downloaded in L1C product in order to use the same atmospheric correction for all of them, by means of the Sen2Cor processor. This processor provides good results in eutrophic waters [8,20,29].

Following [5] results, we used band 5 (705 nm) to estimate turbidity with 20 m of spatial resolution. The reflectance values of band 5 (705 nm) were spatially standardized following Equation (1), where  $x$  is the month datum of sampling station  $i$  pixel,  $\bar{x}$  is the month average of all Albufera lagoon pixels, and  $SD$  is the monthly standard deviation of all Albufera lagoon pixels. The spatially standardized results were transformed into raster format for mapping. The purpose was to characterize the spatial turbidity pattern under different precipitation regime.

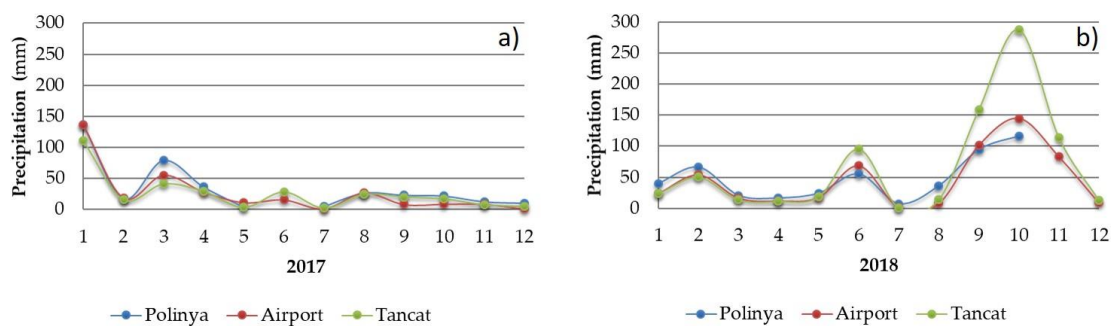
Chl $a$  concentration was estimated from L1C products with the “Case 2 Regional Coast Colour” (C2RCC) processor of the SNAP software. Chl $a$  concentration was mapped to better understand the contribution of phytoplankton to turbidity patterns in the Albufera lagoon.

The Spearman correlation test was used to test the statistical significance of the correlation between remote sensing and in situ data. We contrasted the 2017 and 2018 standardized reflectance values (band 5, 705 nm) with the monthly standardized data of SDD for the complete study period (1998 to 2018) for each sampling station. The remote sensing data of each pixel containing a sampling station was extracted to compare with the historical in situ data.

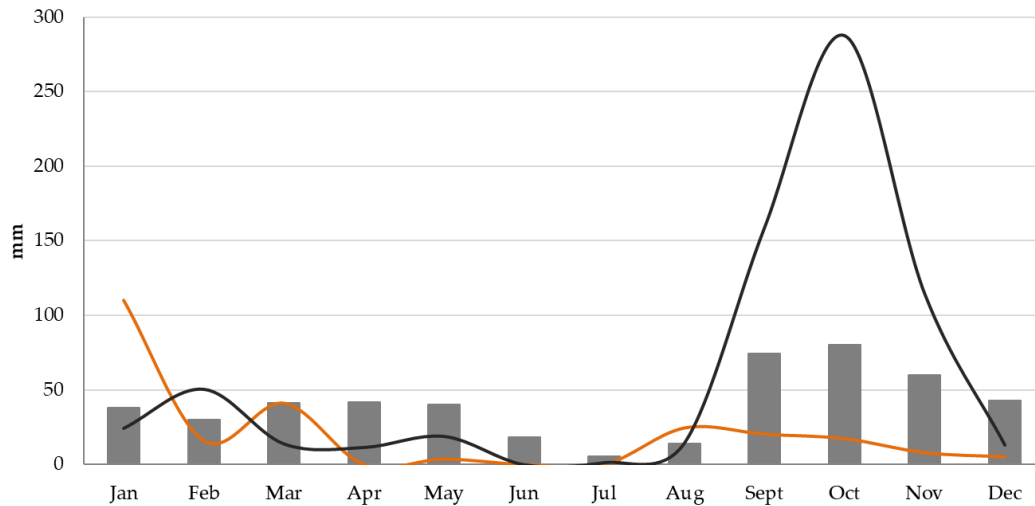
### 3. Results

In Figure 2, monthly precipitation in 2017 and 2018 is compared for the following three meteorological stations: *Polinyà del Xúquer* (south of study area), Valencia Airport (north of study area), and *Tançat de la Pipa* (study area) (Figure 1). The three stations show the same precipitation trend and similar values, except in the autumn of 2018 where *Tançat de la Pipa* experienced more rain. Then, the average monthly precipitation from 1995 to 2018 was built with the average of the nearest stations with available data, Valencia Airport and *Polinyà del Xúquer*. In this Mediterranean-type climate region, the

main rainy period is autumn and the average annual precipitation is 487.7 mm. In Figure 3, the average monthly precipitation is represented (bars) against the monthly precipitation of years 2017 (orange line) and 2018 (black line). The last data was obtained from *Tancat de la Pipa* station. In this station, the total precipitation for 2017 was 307.0 mm being approximately 180 mm lower than average annual precipitation. The total precipitation for 2018 was 709.8 mm, which was more than 200 mm above the average annual precipitation. During the autumn months, September to November, accumulated precipitation was only 45.8 mm in 2017, while in 2018 it was 561.0 mm exceeding the annual average. October 2018 recorded the maximum precipitation with 287.6 mm, with 232.2 mm measured in a single day (18 October 2018). In this area, prevailing wind direction shows a marked seasonal variability. During the warm months the winds of the East and Southeast (winds to the west) prevail, while during the rest of the year the winds of the West prevail (winds to the east), especially from the Southwest (Northwest only in October).



**Figure 2.** Monthly precipitation (a) 2017 and (b) 2018, comparison of the three meteorological stations: *Polinyà del Xúquer* (Polinya), Valencia Airport (Airport), and *Tancat de la Pipa* (Tancat).



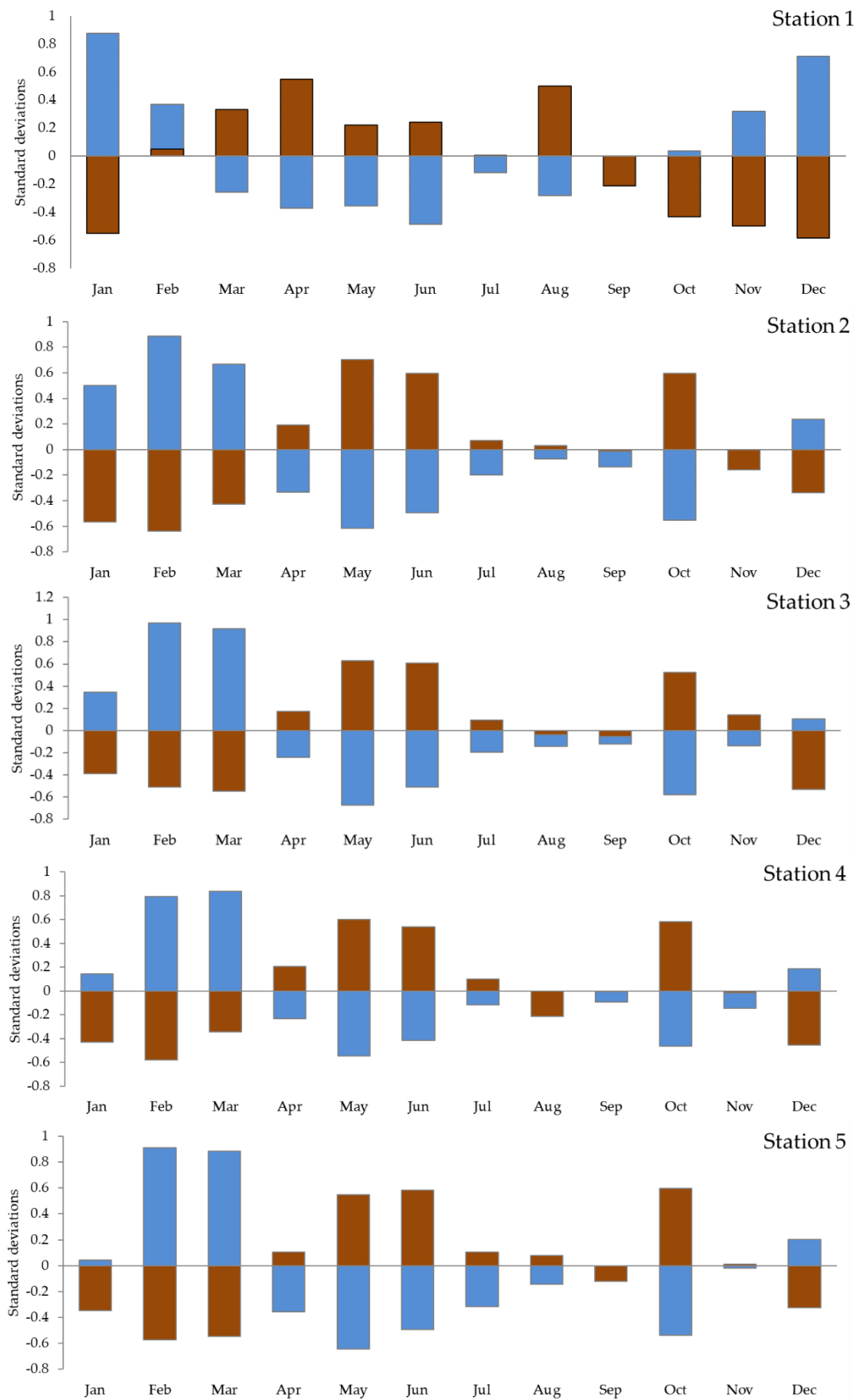
**Figure 3.** Average monthly precipitation (1995 to 2018) calculated from *Polinyà del Xúquer* and Valencia Airport stations (grey bars). Monthly precipitation 2017 (orange line) and 2018 (black line) at *Tancat de la Pipa* station.

Table 2 summarizes data from the in situ monitoring program of the Environment General Subdivision of the Valencian government, from January 2017 to December 2018. There is approximately one measure of each variable (SPM, SDD, and Chl<sub>a</sub>) per month. However, some data is missing; for instance, December 2018 only has SDD data. The highest SPM values were observed in May and June (June 2018 no data available), with values even higher than 100 mg/L, and SDD of about 17 cm in all the sampling stations. The highest Chl<sub>a</sub> values were observed in October 2017 (average about 150 mg m<sup>-3</sup>), and in October and November 2018 (average about 120 and 150 mg m<sup>-3</sup> respectively). To analyze if there is a monthly pattern associated to the irrigation cycle in the Albufera lagoon, we

studied the in situ data of the entire period from 1995 to 2018. In order to detect anomalies above or below the Albufera lagoon baseline, we calculated the standardized monthly averages of SDD (blue bars) and SPM (brown bars) (Figure 4), in the five in situ sampling stations. In this figure, values above zero standard deviations show higher values than the average, and values below zero are lower than the average. SDD and SPM are inversely correlated variables [9,11], so months with high SDD have low SPM. In general, from April to October SPM values are above the average, and the maximum values are observed in May–June and October. However, sampling station 1 shows a different pattern, with SPM values from March to August above the average, and the maximum values in April and August. This can be explained due to East winds during warm months that may have a resuspension and accumulation effect in this shallow area.

**Table 2.** Data from the monitoring program of the Environment General Subdivision of the Valencian government. Suspended particulate matter (SPM), Secchi disk depth (SDD), and chlorophyll *a* (Chl*a*). nd = no data (missing data).

Data	SPM (mg/L)					SDD (cm)					Chl <i>a</i> (mg m <sup>-3</sup> )				
											Station				
	1	2	3	4	5	1	2	3	4	5	1	2	3	4	5
18 January 2017	28	34	40	60	60	35	30	33	25	30	10	3.7	6.9	6.4	3.9
9 February 2017	nd	<1	<1	nd	<1	nd	30	25	nd	25	nd	48.8	39.7	nd	<0.1
14 February 2017	39	41	36	55	81	35	nd	nd	nd	nd	20.1	14.1	15.6	11.1	18.3
20 March 2017	30	23	13	20	28	40	40	45	50	40	43.3	50.9	13.2	2.5	<0.1
3 April 2017	42	38	37	40	40	35	38	40	38	38	30.5	35	8.9	13.8	2.8
9 May 2017	98	nd	90	100	82	nd	nd	nd	nd	nd	46.6	nd	33.1	32.5	22.4
12 June 2017	67	140	97	60	105	18	20	14	17	20	33.9	27.6	88.9	74.7	57.7
11 July 2017	80	48	86	92	86	30	30	25	30	23	42.6	18.2	39.9	51	0.7
7 August 2017	25	nd	35	35	nd	30	30	30	30	30	46.7	nd	49.1	49	nd
11 September 2017	35	35	26	38	43	30	30	30	30	25	<0.1	37.5	<0.1	48.2	<0.1
17 October 2017	nd	76	nd	67	72	30	20	nd	20	25	65.5	157.4	nd	197.9	172
20 November 2017	58	78	84	31	74	30	37.5	30	30	37.5	89	60.6	70.9	69.2	72.6
21 December 2017	nd	41	43	nd	48	32	30	30	nd	30	61.2	73.5	75	nd	160
23 January 2018	52	52	50	nd	60	28	30	35	nd	25	84.3	71.4	82	nd	83.6
19 February 2018	<1	52	82	29	85	23	35	35	50	35	57.1	38.3	67.3	24.3	46.3
1 March 2018	73	64	83	88	103	20	31	30	30	29	163.1	91.1	90.1	98.6	<0.1
17 April 2018	66	116	88	92	90	23	25	23	25	25	<0.1	125.6	67	81.4	45.6
15 May 2018	108	130	130	130	130	30	17	17	20	17	30.6	127.1	167.8	167.2	229.7
13 June 2018	<1	nd	nd	nd	nd	40	25	25	25	25	22.5	nd	nd	nd	nd
11 July 2018	28	22	18	34	40	30	35	35	30	30	101.1	42.9	26.3	41.3	36.2
20 August 2018	22	25	30	35	21	25	35	42	35	37	108.4	26.2	23.5	25.7	23.1
18 September 2018	nd	8	nd	9	25	25	35	nd	35	35	nd	61.6	nd	101.1	38.4
17 October 2018	46	38	53	51	50	nd	30	30	30	30	nd	130.1	92.3	137	117.3
12 November 2018	28	20	20	18	15	nd	30	30	30	30	nd	157.8	143.3	172.1	130.5
11 December 2018	nd	nd	nd	nd	nd	nd	35	40	nd	50	nd	nd	nd	nd	nd
17 December 2018	nd	nd	nd	nd	nd	nd	25	25	25	25	nd	nd	nd	nd	nd
Average	49	49	52	52	58	28	29	29	29	29	55.7	63.7	57.3	67.1	66.6
SD	32	40	38	36	38	14	11	14	15	11	41.9	50	45.8	59	63.1



**Figure 4.** Standardized monthly averages of Secchi disk depth (blue bars) and suspended particulated matter (brown bars) for the period 1995 to 2018, in the five sampling stations of the Albufera lagoon.



Monthly turbidity is mapped in Figure 5 (year 2018) and Figure 6 (year 2017) to better analyze the spatial pattern. Turbidity is represented as standardized reflectances of band 5 (705 nm) from Sentinel 2A and 2B. This reflectance represents turbidity as follows: values in the interval  $(-1, 1)$  indicate average values (blue color); values in the interval  $(1, 1.6)$  are above average conditions (yellow color), and values  $(>1.6)$  are highly anomalous (red color). Applying the spatially standardized anomalies approach is important to be able to detect deviations from the baseline.

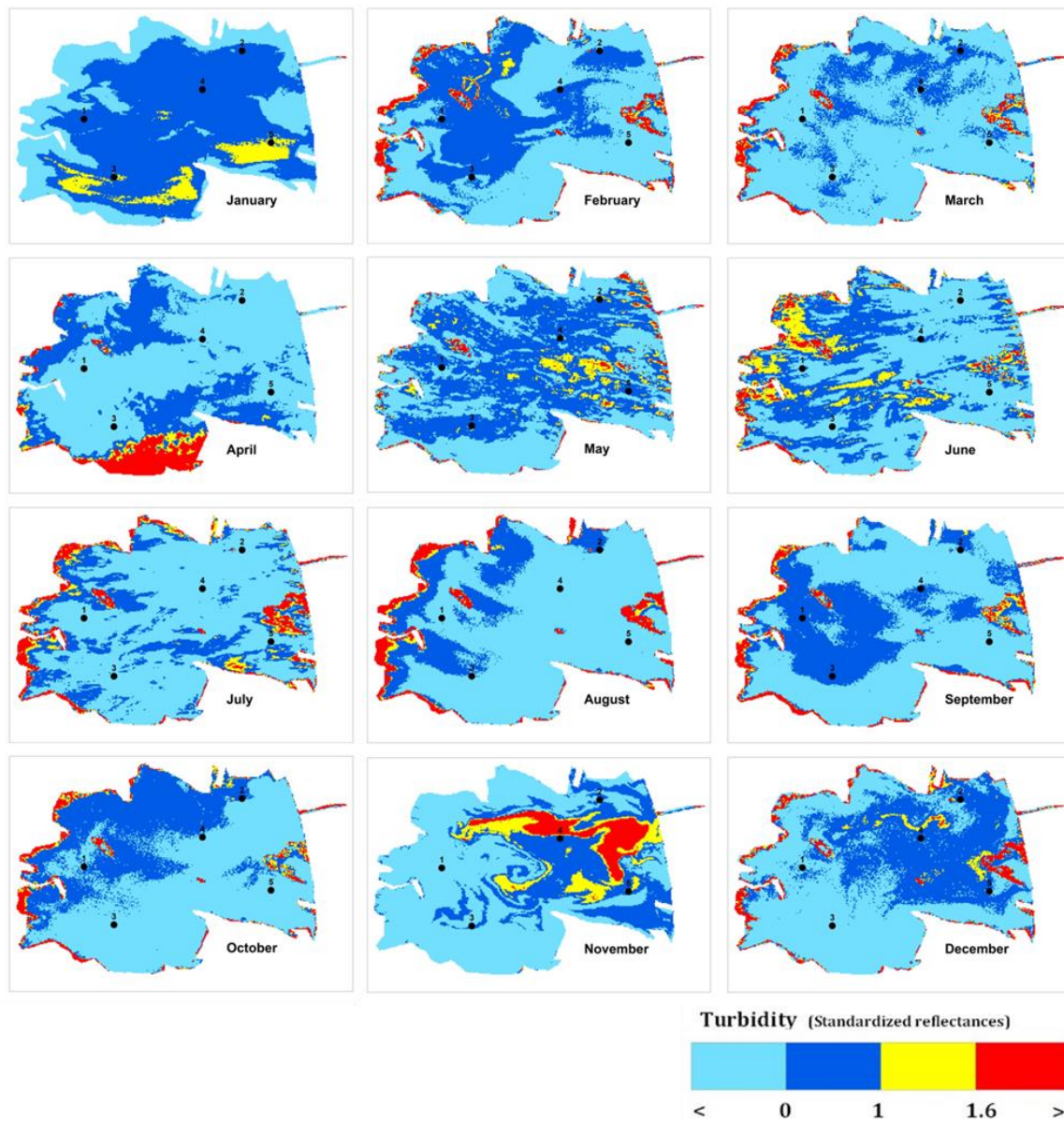


**Figure 5.** Monthly standardized reflectances band 5 (705 nm) from Sentinel 2A and 2B, year 2018, in the Albufera lagoon. Turbidity is represented as follows: values in the interval  $(-1, 1)$  indicate average values; values in the interval  $(1, 1.6)$  are above average conditions, and values  $(>1.6)$  are highly anomalous.

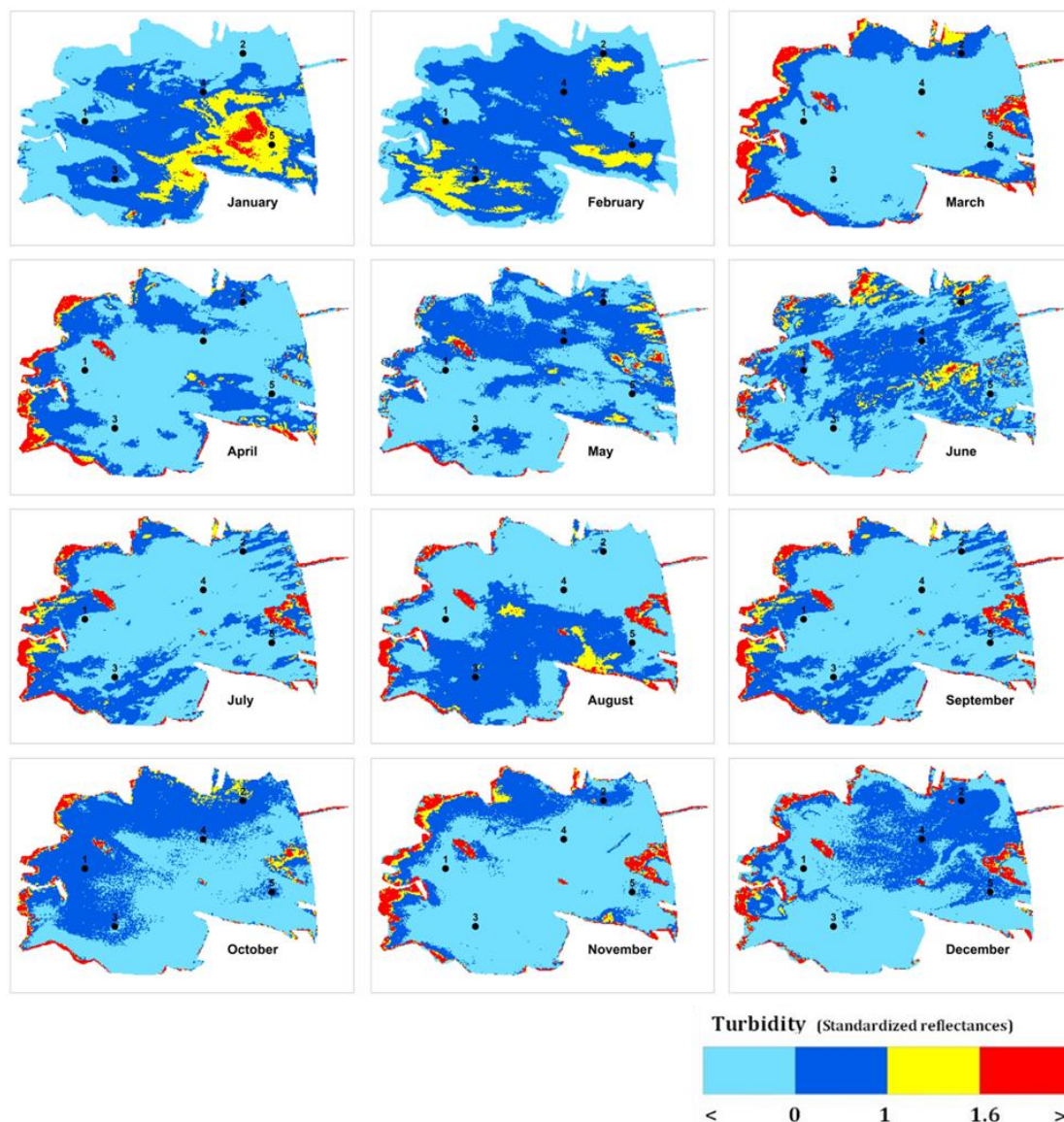


**Figure 6.** Monthly standardized reflectances band 5 (705 nm) from Sentinel 2A and 2B, year 2017, in the Albufera lagoon. Turbidity is represented as follows: values in the interval  $(-1, 1)$  indicate average values; values in the interval  $(1, 2)$  are above average conditions, and values  $(>1.6)$  are highly anomalous.

The spatial distribution of turbidity is quite heterogeneous. Despite the five in situ sampling stations are located all around the lagoon, the high spatial variability is much better captured with remote sensing. The correlation between remote sensing and in situ data was analyzed with the Spearman correlation test. We contrasted the 2017 and 2018 standardized reflectance values (band 5, 705 nm) with the monthly standardized data of SDD for the complete study period (1998 to 2018) for each sampling station (Table 3). We wanted to test if turbidity patterns mapped with remote sensing in the studied years followed the monthly historical pattern. According to  $p$ -values, the correlation was statistically significant ( $p$ -value  $< 0.05$ ) for all sampling stations except sampling station 2, 2018.

It is important to remember that high turbidity values can be due to inorganic particulated matter (sediments) but also to high phytoplankton values [12,13]. Monthly Chl $a$  concentration in the Albufera lagoon is mapped in Figure 7 (year 2018) and Figure 8 (year 2017). Chl $a$  is used a phytoplankton biomass indicator. In general, the highest Chl $a$  values do not coincide with the highest turbidity values, which indicated the major importance of inorganic particles during high turbidity events. For instance, April 2018 is characterized by high Chl $a$  values while turbidity is under the average ( $<0$ ) in nearly all

of the lagoon. Phytoplankton biomass behavior showed differences between a wet year (2018) and a dry year (2017). In 2018, the highest phytoplankton biomass (Chl $a$ ) was observed in April and affected nearly the entire lagoon. In 2017, the highest biomass from May to July also affected nearly the entire lagoon. Both years had a second Chl $a$  maximum in October.

**Table 3.** Correlation between the monthly standardized data of Secchi disk depth and standardized band 5 (705 nm) of Sentinel (for each year  $n = 12$ ).

Sampling Stations	2017		2018	
	Spearman Correlation	$p$ -Value	Spearman Correlation	$p$ -Value
1	0.613	0.034	0.614	0.034
2	0.860	0.000	0.557	0.060
3	0.887	0.000	0.665	0.018
4	0.897	0.000	0.658	0.020
5	0.622	0.031	0.594	0.042

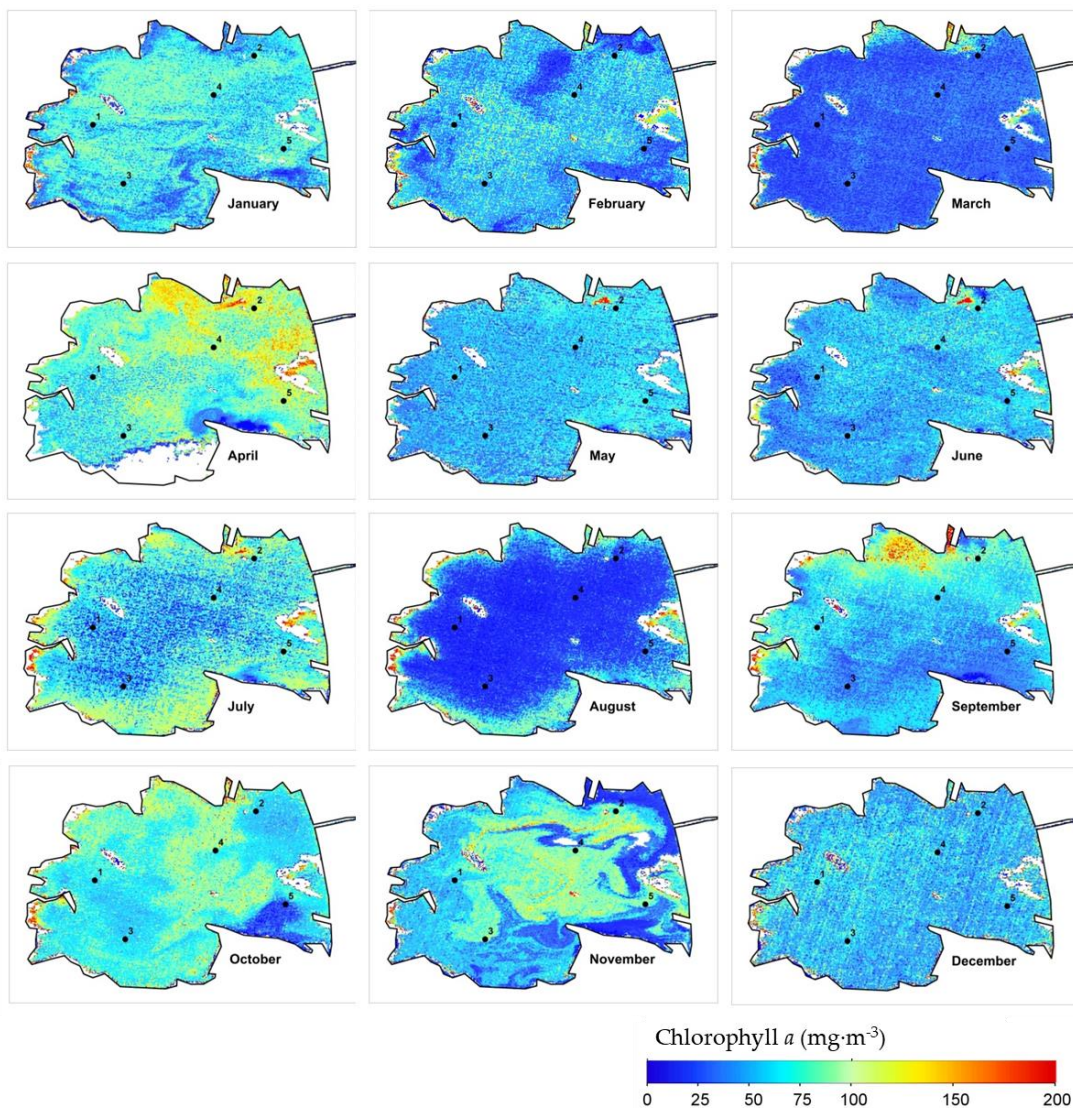


**Figure 7.** Monthly chlorophyll  $a$  concentration in the Albufera lagoon 2018.

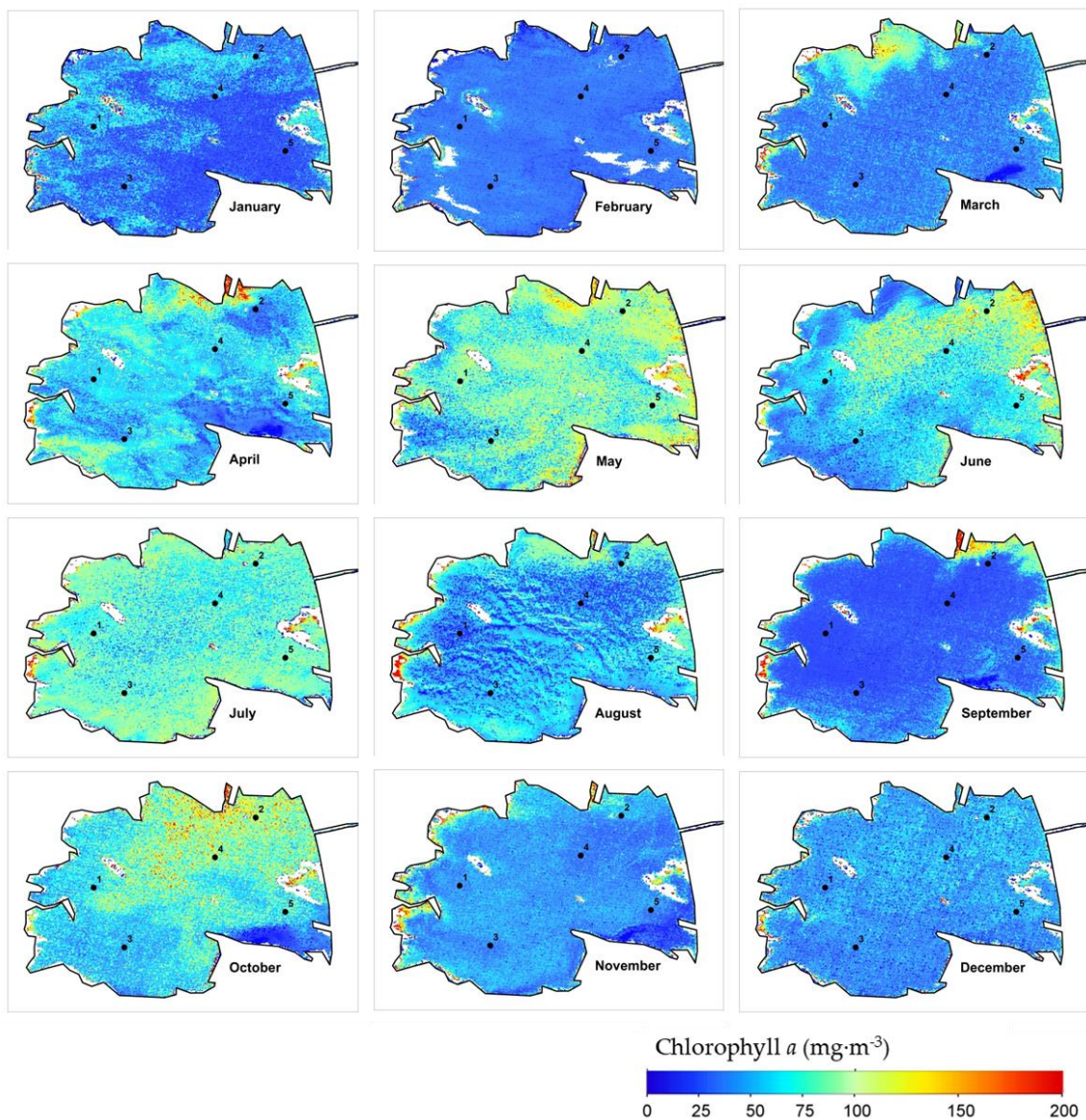


**Figure 8.** Monthly chlorophyll *a* concentration in the Albufera lagoon 2017.

To better analyze temporal variability and the effect of extreme meteorological events, we mapped turbidity and Chl*a* before and after the most important storm of the study period (Figure 9). This storm was on October 18 and total precipitation was 232.2 mm. Before the precipitation, Chl*a* levels were above 75 mg m<sup>-3</sup> in nearly the entire lagoon. After the precipitation, a generalized decrease was observed.

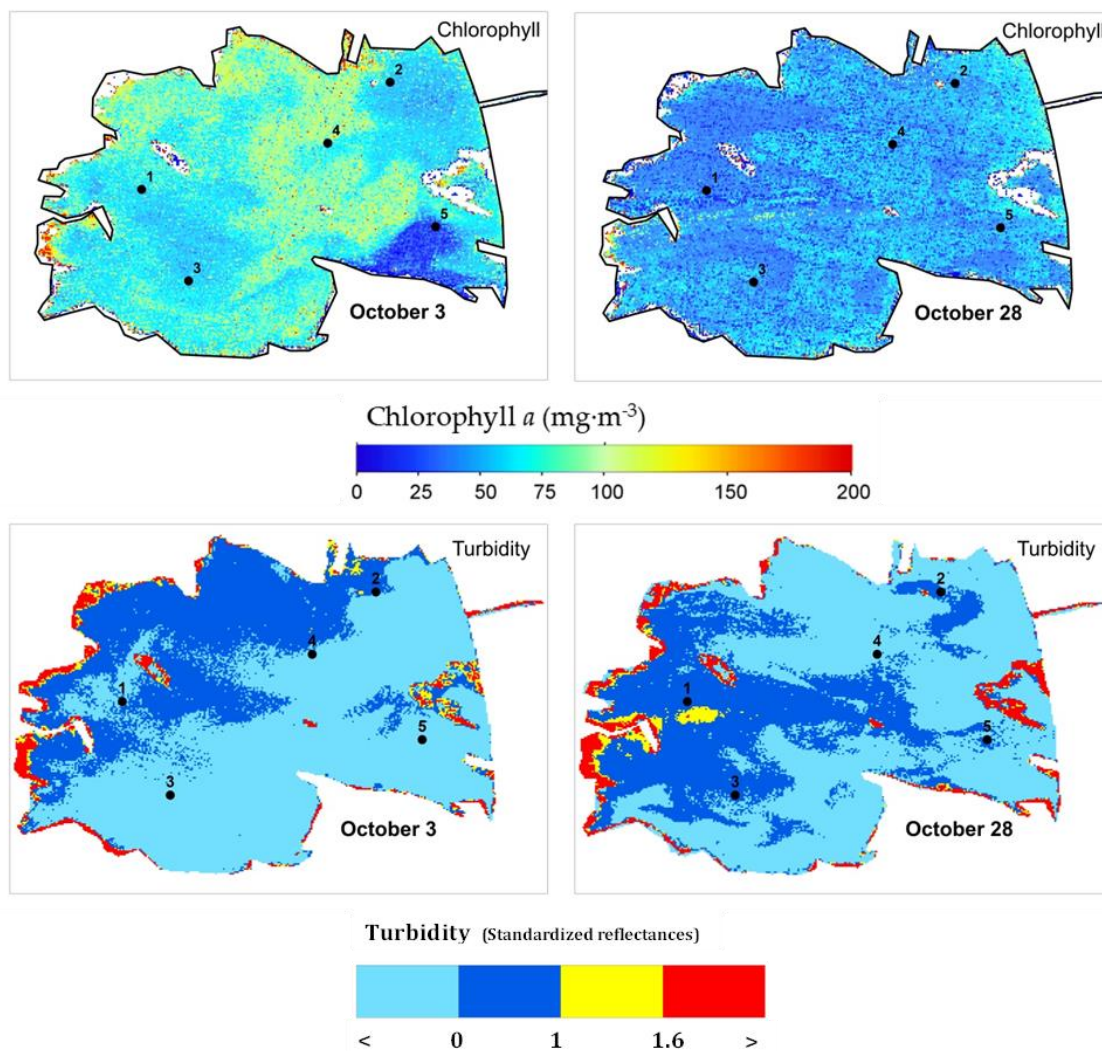


**Figure 9.** Chlorophyll *a* concentration and turbidity before and after a storm in the Albufera lagoon. The storm was on October 18 and total precipitation was 232.2 mm.

#### 4. Discussion

In our study, we applied the standardized anomalies approach to the analysis of spatial and temporal patterns. According to the anomalies theory, the baseline is interpreted as the boundary on which if a value is above it is described as a positive anomaly (or increase), while if a value is below it indicates a negative anomaly (or decrement) [27,28]. The baseline was calculated from the period 1995 to 2018, the available historical data that defines the recent average behavior. Thanks to that analysis, in Figure 4, we can clearly distinguish the seasonal pattern. The temporal pattern in the Albufera lagoon is highly dependent on the rice cycle regulation of water inflows. SPM is higher from April to October in all sampling stations (except sampling station 1 from March to August), and thus the SDD is lower from April to October (Figure 4). The rice growing season is approximately from March–April to September. This period is characterized by high residence time of water in the lagoon since floodgates are closed and freshwater inputs are minimum [3]. In September, floodgates are opened to dry the fields for harvesting. The rainy season starts in September in this Mediterranean area when the floodgates are open; this favors water renewal. During the study period, from 1995 to 2018, the lowest water transparency is in May–June and October in sampling stations 2 to 5. Sampling station 1 exhibits slightly different behavior. A lower water transparency is maintained from March to September and transparency only shows a recovery during November to January. This station is located in the western area of the lagoon, which is the shallowest part (<0.9 m).

In general, the turbidity temporal and spatial pattern is similar in a wet year (2018, Figure 5) than in a dry year (2017, Figure 6). Thanks to the spatially standardized anomalies approach, it is important easy to detect deviations from the baseline. The highest turbidity values were observed on the west shore of the lagoon during most of the year. This agrees with the lagoon hydrological sectors proposed by [30]. According to them, the Northwest and West sectors have the lowest water circulation, while the Northeast and Southeast areas have the highest due to the proximity of the gates. The highest *Chl<sub>a</sub>* values are also observed very close to the western shore, as observed also by [3], but also the northern shore reaches very high values.

The spatial distribution of turbidity observed in Figures 5 and 6 is closely related to meteorological events. From September to November 2018, several heavy rain events carried more sediments to the lagoon through surface runoff. In [22] the authors explained that heavy storms were one of the main factors explaining the variation in the limnology of the Albufera lagoon. Storms may last only a few hours in this Mediterranean area, and a single storm could double the annual mean rainfall (e.g., October 2018 precipitation was higher than 2017 annual precipitation). During these storms, the potential for soil infiltration is low, so runoff is very important. We observed high turbidity both in the western sector of the lagoon and near the outflowing channels (eastern sector). In these areas, the phytoplankton and sediments can be transported to the sea because the floodgates (Golas) are open. These high turbidity values are mapped in yellow color (values above the average) and in red (highly anomalous values). From July to September, during the rice growing season, when freshwater inflows to the lagoon are greatly reduced, the most important variable is east wind. The wind dominant direction from sea to land causes the accumulation of suspended material in the western area of the lagoon. In April a false anomaly is observed, which was due to cloud presence. The study images were selected taking into account the lowest cloud coverage to avoid these interferences, but no better image was available in April 2018.

In recent decades, a clear water phase (CWP) has been observed yearly, but it does not show a regular pattern, either temporally or spatially in the lagoon [30,31]. During this phase cyanobacteria plankton is substituted by other microalgae, especially diatoms, which are consumed by filter-feeders such *Daphnia magna* [31]. The authors of [8] studied with Landsat images a CWP event that happened in March 2000. They observed that the re-eutrophication process started from the northwest shoreline, which is the area with lowest circulation [30]. A CWP was reported in January 2017 [7]. As shown in Figure 5, we observed an area of high transparency next to the west shoreline and a highly turbid area in the southeast part of the lagoon. In this month, an important rain event was the most possible cause of sediment transport towards the floodgates. In [7] the authors found two annual minima of cyanobacteria (March and September), which is the dominant phytoplankton in this hypereutrophic lagoon. These minima coincide with the maximum area of transparency in Figure 5, and with low *Chl<sub>a</sub>* values in Figures 7 and 8. However, in 2017 the lowest *Chl<sub>a</sub>* values were detected in February. The authors of [7] observed one cyanobacteria maximum in May. Then, they describe a sharp decline in primary production that contrasts with other authors such as [3], who found that *Chl<sub>a</sub>* concentrations increase from May to August 2006 due to the low water circulation. We can appreciate in Figures 4 and 5 an increase in turbidity from March to May, and a decrease in turbidity from May to August, which is more marked in 2018 (Figure 5). In our results, the *Chl<sub>a</sub>* pattern is different each studied year, in 2017 high *Chl<sub>a</sub>* levels are constant from May to July, while in 2018 there is an important decrease after April. The main difference between both years was an important precipitation event of 82.6 mm on 3 June 2018. This shows the importance of meteorological events on the lagoon dynamics. To analyze this further, Figure 9 shows *Chl<sub>a</sub>* concentration before and after the most important precipitation in October 2018. The decrease in *Chl<sub>a</sub>* after the storm and the water quality improvement can be explained by rapid flushing. If we compare Figures 5 and 6 with Figures 7 and 8, the highly anomalous values of turbidity cannot be attributed to *Chl<sub>a</sub>*, which suggests the importance of inorganic particulated matter, and indicates sediment transport.

The analysis of turbidity gives information about organic and inorganic suspended materials, that is, about phytoplankton and inorganic particles. Previous remote sensing research [8,32] focuses mainly on Chl $a$  study, which is an indicator of phytoplankton biomass. Our study of turbidity patterns provides important supplementary information to those previous studies. The authors of [30] demonstrated that flushing pulses are key to improve water quality and to remediate eutrophication. In our study, we demonstrated that during important rain events the turbidity pattern shows higher values towards the floodgates “Golas”. Then, it is important that during rain events the connection between the lagoon and the sea remains open to allow sediment discharge and prevent clogging of the lagoon. Dredging the lagoon to remove the sediments has been considered by the managers for several years to solve both eutrophication and clogging problems [33]. However, dredging is a desperate measure, very costly, and with environmental consequences. An improved water management, with increased flushing pulses frequency would be a good management measure that could help in alleviating not only eutrophication problems but also lagoon clogging. For that reason, it is essential to maintain the freshwater inflow to this lower part of the Júcar and Turia rivers. In recent years, three constructed wetlands have been developed in the Albufera lagoon (*Tancat de la Pipa*, *Tancat de Mília*, and *Estany de la Plana*), but their functioning is not maximizing the removal of phytoplankton, phosphorus, and nitrogen [6,34]. A better understanding of turbidity patterns can provide relevant information to choose the most suitable location for future restoration measures.

## 5. Conclusions

In our study, we applied the standardized anomalies approach to the analysis of spatial and temporal patterns of turbidity. This methodology allows comparing variables measured with different units, such as SPM and SDD in this study, and detecting deviations from a baseline. Thanks to this approach we can define the seasonal pattern of turbidity, which is not possible by the analysis of an isolated year or a reduced number of study years. In addition, we can define the areas with the highest values above the spatial baseline, which means we can identify the lagoon areas with the most anomalous values.

Turbidity patterns in the Albufera lagoon show a similar trend in wet and dry years, which is mainly linked to the irrigation practice of rice paddies. High turbidity periods are linked to higher water residence time and closed floodgates. However, precipitation and wind also play an important role in the spatial distribution of turbidity. During storm events, phytoplankton and sediments are discharged to the sea, if the floodgates remain open. Fortunately, the rice harvesting season, when the floodgates are open, coincides with the beginning of the rainy period. Nevertheless, this is a lucky coincidence. It is important to develop a conscious management of floodgates, because having them closed during rain events can have several negative effects both for the lagoon and for the receiving coastal waters and ecosystem. Non-discharged solids may accumulate in the lagoon worsening the clogging problems, and the beaches next to the receiving coastal waters will not receive an important load of solids to nourish them.

**Author Contributions:** Conceptualization, methodology, investigation, data curation and writing-original draft preparation M.-T.S.-F and J.A.A.-M.; software and formal analysis J.A.A.-M.; resources and funding acquisition M.-T.S.-F; writing review and editing M.-T.S.-F. and J.E. Visualization and supervision M.-T.S.-F, J.E. and E.S.-D.-Á.

**Funding:** María-Teresa Sebastián-Frasquet was a beneficiary of the CAS18/00107 post-doctoral research grant, supported by the Spanish Ministry of Education Culture and Sports during her stay at the Universidad Autónoma de Baja California (Mexico); image processing was developed partially during her stay. J.A.A.-M. was a beneficiary of the doctorate scholarship with the announcement number 291025, supported by the Council of Science and Technology of Mexico (CONACYT by its acronym in Spanish).

**Acknowledgments:** The authors want to thank María Sahuquillo, from the Environment General Subdivision of the Valencian government, and Paloma Mateache, Natural Park director for their insightful knowledge of the lagoon dynamics and help in interpreting the results. The authors also want to thank the anonymous reviewers who helped to improve the original manuscript.

**Conflicts of Interest:** The authors declare no conflict of interest. The funders had no role in the design of the study; in the collection, analyses, or interpretation of data; in the writing of the manuscript, or in the decision to publish the results.

## References

1. Riera, R.; Tuset, V.M.; Betancur-R, R.; Lombarte, A.; Marcos, C.; Pérez-Ruzafa, A. Modelling alpha-diversities of coastal lagoon fish assemblages from the Mediterranean Sea. *Prog. Oceanogr.* **2018**, *165*, 100–109. [[CrossRef](#)]
2. Sebastiá-Frasquet, M.-T.; Altur, V.; Sanchis, J.-A. Wetland Planning: Current Problems and Environmental Management Proposals at Supra-Municipal Scale (Spanish Mediterranean Coast). *Water* **2014**, *6*, 620–641. [[CrossRef](#)]
3. Doña, C.; Chang, N.B.; Caselles, V.; Sánchez, J.M.; Camacho, A.; Delegido, J.; Vannah, B.W. Integrated satellite data fusion and mining for monitoring lake water quality status of the Albufera de Valencia in Spain. *J. Environ. Manag.* **2015**, *151*, 416–426. [[CrossRef](#)]
4. Gernez, P.; Lafon, V.; Lerouxel, A.; Curti, C.; Lubac, B.; Cerisier, S.; Barillé, L. Toward Sentinel-2 High Resolution Remote Sensing of Suspended Particulate Matter in Very Turbid Waters: SPOT4 (Take5) Experiment in the Loire and Gironde Estuaries. *Remote Sens.* **2015**, *7*, 9507–9528. [[CrossRef](#)]
5. Caballero, I.; Navarro, G.; Ruiz, J. Multi-platform assessment of turbidity plumes during dredging operations in a major estuarine system. *Int. J. Appl. Earth Obs. Geoinf.* **2018**, *68*, 31–41. [[CrossRef](#)]
6. Onandia, G.; Gudimov, A.; Miracle, M.R.; Arhonditsis, G. Towards the development of a biogeochemical model for addressing the eutrophication problems in the shallow hypertrophic lagoon of Albufera de Valencia, Spain. *Ecol. Inform.* **2015**, *26*, 70–89. [[CrossRef](#)]
7. Sòria-Perpinyà, X.; Vicente, E.; Urrego, P.; Pereira-Sandoval, M.; Ruíz-Verdú, A.; Delegido, J.; Soria, J.M.; Moreno, J. Remote sensing of cyanobacterial blooms in a hypertrophic lagoon (Albufera of València, Eastern Iberian Peninsula) using multitemporal Sentinel-2 images. *Sci. Total Environ.* **2020**, *698*, 134305. [[CrossRef](#)] [[PubMed](#)]
8. Sòria-Perpinyà, X.; Urrego, P.; Pereira-Sandoval, M.; Ruiz-Verdú, A.; Peña, R.; Soria, J.M.; Delegido, J.; Vicente, E.; Moreno, J. Monitoring the ecological state of a hypertrophic lake (Albufera of València, Spain) using multitemporal Sentinel-2 images. *Limnetica* **2019**, *38*, 457–469.
9. Güttler, F.N.; Niculescu, S.; Gohin, F. Turbidity retrieval and monitoring of Danube Delta waters using multi-sensor optical remote sensing data: An integrated view from the delta plain lakes to the western–northwestern Black Sea coastal zone. *Remote Sens. Environ.* **2013**, *132*, 86–101. [[CrossRef](#)]
10. Quang, N.H.; Sasaki, J.; Higa, H.; Huan, N.H. Spatiotemporal Variation of Turbidity Based on Landsat 8 OLI in Cam Ranh Bay and Thuy Trieu Lagoon, Vietnam. *Water* **2017**, *9*, 570. [[CrossRef](#)]
11. Kari, E.; Kratzer, S.; Beltrán-Abaunza, J.M.; Harvey, E.T.; Vaičiute, D. Retrieval of suspended particulate matter from turbidity-model development, validation, and application to MERIS data over the Baltic Sea. *Int. J. Remote Sens.* **2017**, *38*, 1983–2003. [[CrossRef](#)]
12. Kuhn, C.; de Matos Valerio, A.; Ward, N.; Loken, L.; Oliveira Sawakuchi, H.; Kampel, M.; Richey, J.; Stadler, P.; Crawford, J.; Striegl, R.; et al. Performance of Landsat-8 and Sentinel-2 surface reflectance products for river remote sensing retrievals of chlorophyll-a and turbidity. *Remote Sens. Environ.* **2019**, *224*, 104–118. [[CrossRef](#)]
13. Liu, H.; Li, Q.; Shi, T.; Hu, S.; Wu, G.; Zhou, Q. Application of Sentinel 2 MSI Images to Retrieve Suspended Particulate Matter Concentrations in Poyang Lake. *Remote Sens.* **2017**, *9*, 761. [[CrossRef](#)]
14. Erena, M.; Domínguez, J.A.; Aguado-Giménez, F.; Soria, J.; García-Galiano, S. Monitoring Coastal Lagoon Water Quality through Remote Sensing: The Mar Menor as a Case Study. *Water* **2019**, *11*, 1468. [[CrossRef](#)]
15. Caballero, I.; Stumpf, R.P.; Meredith, A. Preliminary Assessment of Turbidity and Chlorophyll Impact on Bathymetry Derived from Sentinel-2A and Sentinel-3A Satellites in South Florida. *Remote Sens.* **2019**, *11*, 645. [[CrossRef](#)]
16. Vanhellemont, Q.; Ruddick, K. Acolite for Sentinel-2: Aquatic applications of MSI imagery. In Proceedings of the 2016 ESA Living Planet Symposium, Prague, Czech Republic, 9–13 May 2016.
17. IOCCG. *Remote Sensing of Ocean Colour in Coastal, and Other Optically-Complex, Waters*; Reports of the International Ocean-Colour Coordinating Group, No. 3; Sathyendranath, S., Ed.; IOCCG: Dartmouth, NS, Canada, 2000.



18. Toming, K.; Kutser, T.; Laas, A.; Sepp, M.; Paavel, B.; Nõges, T. First experiences in mapping lake water quality parameters with Sentinel-2 MSI imagery. *Remote Sens.* **2016**, *8*, 640. [[CrossRef](#)]
19. Soria, J.M.; Miracle, M.R.; Vicente, E. Aporte de nutrientes y eutrofización de la Albufera de Valencia. *Limnetica* **1987**, *3*, 227–242.
20. Soria, X.; Delegido, J.; Urrego, E.P.; Pereira-Sandoval, M.; Vicente, E.; Ruíz-Verdú, A.; Moreno, J. Validación de algoritmos para la estimación de la clorofila-a con Sentinel-2 en la Albufera de València. In Proceedings of the XVII Congreso de la Asociación Española de Teledetección, Murcia, Spain, 3–7 October 2017; pp. 289–292.
21. Usaquén Perilla, O.L.; García Gómez, A.; Álvarez Díaz, C.; Revilla Cortezón, J.A. Methodology to assess sustainable management of water resources in coastal lagoons with agricultural uses: An application to the Albufera lagoon of Valencia (Eastern Spain). *Ecol. Indic.* **2012**, *13*, 129–143. [[CrossRef](#)]
22. Soria, J.M.; Vicente, E.; Miracle, M.R. The influence of flash floods on the limnology of the Albufera of Valencia lagoon (Spain). *Int. Ver. Theor. Angew. Limnol. Verh.* **2000**, *27*, 2232–2235. [[CrossRef](#)]
23. Romo, S.; García-Murcia, A.; Villena, M.J.; Sanchez, V.; Ballester, A. Phytoplankton trends in the lake of Albufera de Valencia and implications for its ecology, management, and recovery. *Limnetica* **2008**, *27*, 11–28.
24. Vicente, E.; Miracle, M.R. The coastal lagoon Albufera de Valencia: An ecosystem under stress. *Limnetica* **1992**, *8*, 87–100.
25. Wang, S.; Lee, Z.; Shang, S.; Li, J.; Zhang, B.; Lin, G. Deriving inherent optical properties from classical water color measurements: Forel-Ule index and Secchi disk depth. *Opt. Express* **2019**, *27*, 7642–7655. [[CrossRef](#)] [[PubMed](#)]
26. Wernand, M.R. On the history of the Secchi disc. *J. Eur. Opt. Soc.-Rapid Publ.* **2010**. [[CrossRef](#)]
27. Santamaría-del-Ángel, E.; Sebastia-Frasquet, M.T.; Gonzalez-Silvera, A.; Aguilar-Maldonado, J.; Mercado-Santana, A.; Herrera-Carmona, J. Uso Potencial de las Anomalías Estandarizadas en la Interpretación de Fenómenos Oceanográficos Globales a Escalas Locales. In *Costas y Mares Mexicanos: Construyendo la Línea Base para su Futuro Sostenible, Oceanografía Fisicoquímica*; Rivera-Arriaga, E., Sánchez-Gil, P., Gutiérrez, J., Eds.; EPOMEX: Campeche, Mexico; Universidad Autónoma de Colima: Colima, Mexico, 2019.
28. Aguilar-Maldonado, J.A.; Santamaría-del-Ángel, E.; Gonzalez-Silvera, A.; Sebastián-Frasquet, M.T. Detection of Phytoplankton Temporal Anomalies Based on Satellite Inherent Optical Properties: A Tool for Monitoring Phytoplankton Blooms. *Sensors* **2019**, *19*, 3339. [[CrossRef](#)] [[PubMed](#)]
29. Pereira-Sandoval, M.; Ruescas, A.; Urrego, P.; Ruiz-Verdú, A.; Delegido, J.; Tenjo, C.; Soria-Perpinyà, X.; Vicente, E.; Soria, J.; Moreno, J. Evaluation of Atmospheric Correction Algorithms over Spanish Inland Waters for Sentinel-2 Multi Spectral Imagery Data. *Remote Sens.* **2019**, *11*, 1469. [[CrossRef](#)]
30. Soria, J.M. Past, present and future of la Albufera of Valencia Natural Park. *Limnetica* **2006**, *25*, 135–142.
31. Miracle, M.R.; Sahuquillo, M. Changes of life-history traits and size in *Daphnia magna* during a lear-water phase in a hypertrophic lagoon (Albufera of Valencia, Spain). *Int. Ver. Theor. Angew. Limnol. Verh.* **2002**, *28*, 1203–1208.
32. Sòria-Perpinyà, X.; Miracle, M.R.; Soria, J.; Delegido, J.; Vicente, E. Remote sensing application for the study of rapid flushing to remediate eutrophication in shallow lagoons (Albufera of Valencia). *Hydrobiologia* **2019**, *829*, 125–132. [[CrossRef](#)]
33. Rodrigo, M.A.; Alonso-Guillén, J.A. Assessing the potential of Albufera de València Lagoon sediments for the restoration of charophyte meadows. *Ecol. Eng.* **2013**, *60*, 445–452. [[CrossRef](#)]
34. Martín, M.; Oliver, N.; Hernández-Crespo, C.; Gargallo, S.; Regidor, M. The use of free water surface constructed wetland to treat the eutrophicated waters of lake L'Albufera de Valencia (Spain). *Ecol. Eng.* **2013**, *50*, 52–61. [[CrossRef](#)]

